**Detector Tests**
Gas–Silicon Hybrids

Author: A.St.J. Murphy
Date: 1 February 1993

# Notes on the Performance of the new Gas – Silicon Hybrid detectors

A. St. J. Murphy
School of Physics and Space Research
University of Birmingham, B15 2TT, U.K.

**Abstract**

Initial analysis of the data taken at Daresbury in November 1992 (Proposal 874) has revealed that the position response of the new gas - silicon hybrid detectors may be rather better than expected. In particular, the 0.1 mm diameter wires of the anode and earthing grids have been cleanly observed, and the effect of 120 torr of isobutane gas upon this position resolution has been shown to be negligible.

## Introduction.

In November 1991, an experiment was performed at the NSF to search for possible molecular states in $^{48}$Cr, such as the $^{16}$O - $^{16}$O - $^{16}$O chain configuration. This experiment hoped to populate states in $^{48}$Cr via a $^{24}$Mg + $^{24}$Mg entrance channel, at energies of 150 and 170 MeV$_{lab}$, and then to observe decays to three heavy fragments by detection in coincidence of any two. The detector array utilised the old $10 \times 10$ mm position sensitive detectors (psd's) that have served *Charissa* for the last five years or so. Analysis of the data taken revealed little or no evidence for the breakup of $^{48}$Cr into any heavy ion chain states [1], but the observation of a very strong reaction coming from a thin layer of carbon build-up on the target seriously hampered these conclusions. Estimates of an upper limit for the double differential cross-section were made for a number of exit channels, and although these were small, it was thought possible that the true reaction cross-sections might exist at lower levels. Therefore, a second experiment was performed with the aim of improving the sensitivity of these measurements. These improvements included the use of a cold trap to reduce any carbon build-up, and the use of the new gas-silicon hybrid detector telescopes to increase the detection efficiency.

The first stages of the analysis of this new data have now been completed, and this has shown that the performance of new detectors is as good, if not better than expected.

## The Gas-Silicon Hybrid Detectors.

A schematic drawing of one of the new detectors is show in figure 1. The detectors consisted of a gas $\Delta E$ detector together with a silicon $E$ detector. The gas detector was operated with isobutane gas at a pressure of 120 torr, constrained within a thin (6$\mu$m) mylar window. This inside of this window had a layer of aluminium evaporated on to it, allowing it to be earthed to smooth the electric field gradients within the detector. The recommended bias voltage for these detectors is about 2.5 V/torr/cm, and therefore the detectors were operated at a bias of 600 V. The silicon $E$ detector was a 50 $\times$ 50 mm single-sided strip detector with 16 strips. Signals were taken from both ends of each strip, and the strips were resistive, allowing charge division along the length of the strip. It was predicted that this position sensitivity would be superior to the $\approx$3 mm sensitivity that would be achieved in the perpendicular direction given by the identity of the strip, and therefore the strips were placed parallel to the plane of detection. The thickness of the silicon detector was chosen to be enough to stop all incident ions of interest, in this case requiring a 300 $\mu$m thick silicon detector.

The main reason for using these new detectors is demonstrated by figure 2, which shows a "Monte Carlo"calculation of the comparative detection efficiency of the old and the new detector arrays, with respect to the generation of $E_{rel}$ spectra. This assumes that the old detectors were placed at 120 mm from the target, and that the new detectors are used with the silicon at 240mm, and in both cases at angles optimised for the detection of events resulting from the $^{24}$Mg($^{24}$Mg,$^{16}$O,$^{16}$O)$^{16}$O reaction. Despite the detectors being twice as far back from the target, there is still approximately a ten-fold increase in the detection efficiency, and since the dominant contribution to the resolution of $E_{rel}$ comes from the angular resolution, this increased target – detector separation is beneficial. However, this apparent improvement in the angular resolution may only realised if the intrinsic position sensitivity of the new silicon detectors can be shown to be at least as good as that of the old psd's.

## Data Analysis.

During the experiment only limited calibration of the apparatus used could be made. The later off-line analysis has allowed such factors as given below to be addressed.

**1** Gain drifts in electronics.

**2** Correction of any adc offsets.

**3** Check for adc non-linearities.

**4** Initial gain-matching between the ends of each strip.

The check for any gain drifts was achieved by comparing the centroid of the pulser peak in a particular spectrum, and seeing if that changed from one run to another. No significant variations were found for a number of spectra.

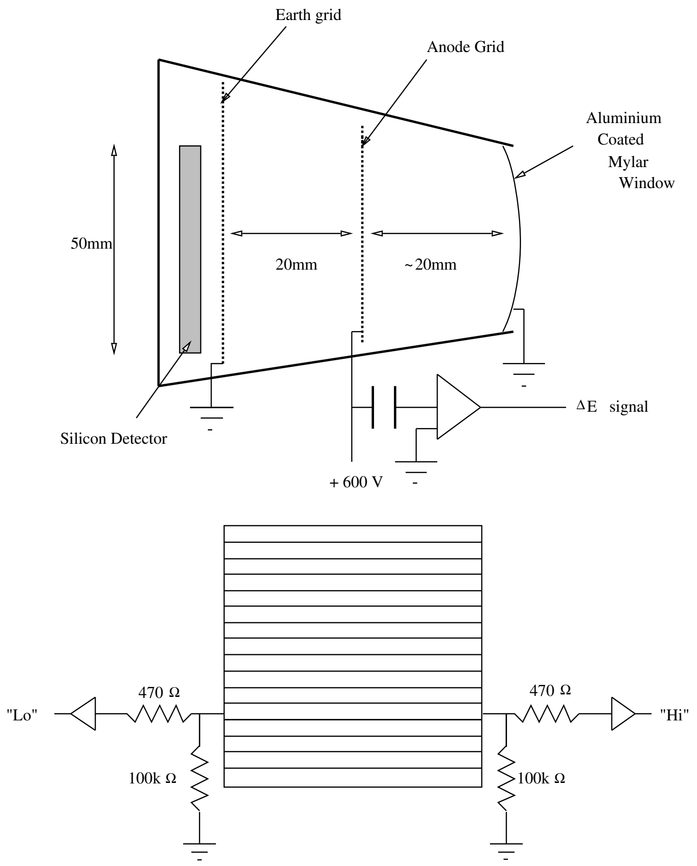


Figure 1: Schematic diagram of a gas-silicon hybrid detectors. The bottom figure describes the biasing of the strip detector.

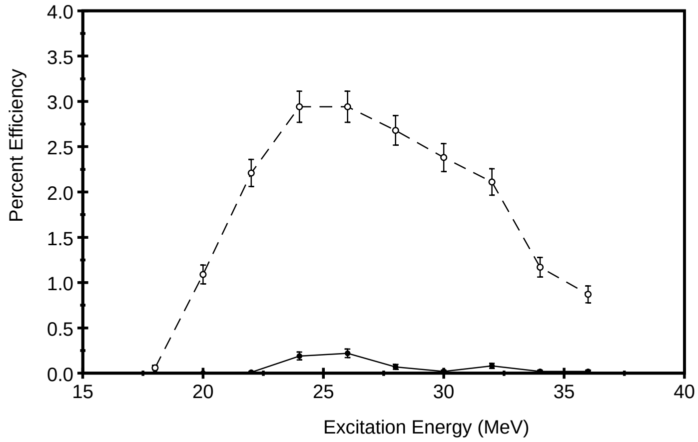


Figure 2: A comparison of the efficiency profiles for the Daresbury 1991 experiment (solid line) and the more recent follow-up experiment (dashed line).

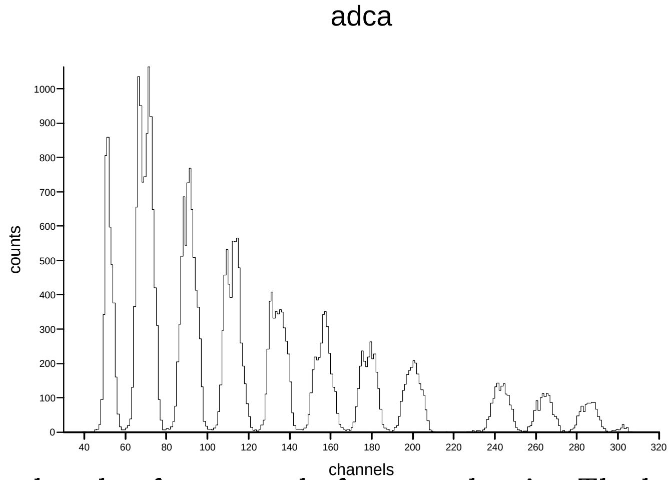

Figure 3: Raw adc value for one end of a central strip. The large peaks are due to the calibration mask.

Two runs were performed at the end of the experiment which consisted of matchsticks data. This has been used to check for non-linearities and for offsets in the adc response. No significant non-linearities have been observed, but nearly all of the adc's appear to have a significant offset. These offsets have been recorded, and are subtracted from the value of the adc in any subsequent sorting.

As yet, a full gain-matching of the ends of each strip has not been performed. However, for all the results given in this report a gain-matching has been made by use of a software variable that multiplies the adc value of the signal from one of the ends of the strip. A more comprehensive gain-matching is probably the next stage of analysis.

## Results.

The first spectra were generated by simply incrementing each of the adc's into a 4096 spectrum. An example is shown in figure 3, which is the "high" signal from the middle strip of the beam-right detector for 70 MeV $^{16}$O ions off a 100$\mu$g/cm$^2$ $^{197}$Au target. Since the ions are nearly mono-energetic, this forms a position spectrum. The ten large peaks are due to the calibration mask, but it appears that each of the peaks is further divided into two or three smaller peaks, the amplitude of these oscillations being much larger than statistical expectations.

A similar spectrum, but for data taken without the mask present (170 MeV $^{24}$Mg ions off a flash - gold target) is shown in figure 4, and these oscillations can now be seen right across the detector face. A true position spectrum generated by plotting high/(high+low) reveals this structure even more clearly (see figure 5). It was noticed that there were of the order of 50 oscillations, and hence it was suggested that they may be due to either one or both of the grids shown in figure 1.

This view is reinforced by figure 6, which is an energy spectrum of the signals from one end of a strip of the same detector. The data was taken by removing the silicon detector from the hybrid casing, and illuminating it with near mono-energetic 5.5 MeV alpha-particles from an $^{241}$Am source. Again, since the alpha-particles are near mono-energetic, this forms a position spectrum, and although the edges of the detector appear much smoother suggesting a worse position resolution, there is a total absence of the previous dips.

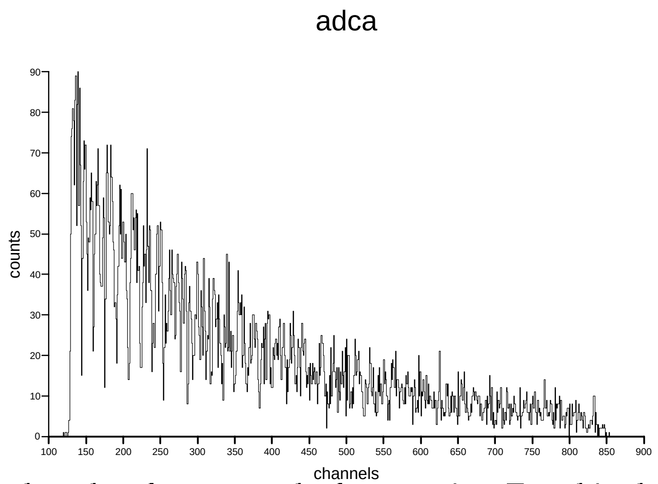


Figure 4: Raw adc value for one end of one strip. For this data the calibration mask has been removed and so the entire detector face is visible.

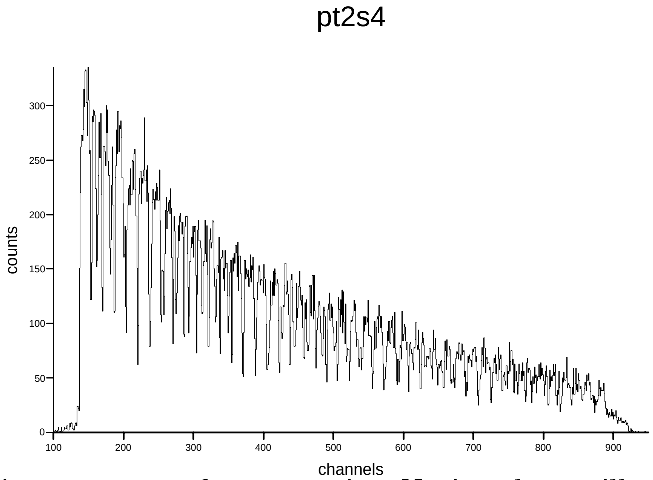


Figure 5: Position spectrum for one strip. Notice the oscillations spanning the entire detector.

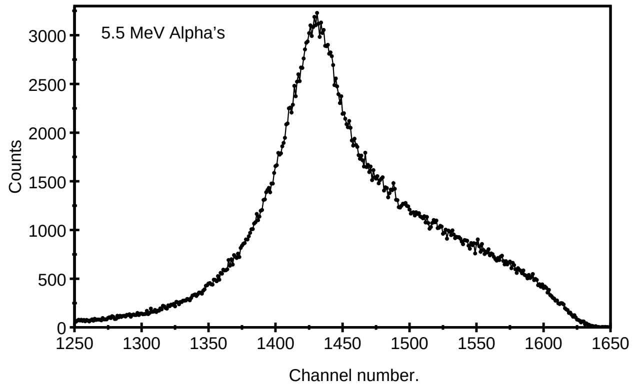


Figure 6: Raw adc signal for data taken with an $^{241}$Am alpha-particle source with the grids not present. The smoothness of the spectrum reinforces the view that the grids are responsible for the dips observed in figure 5.

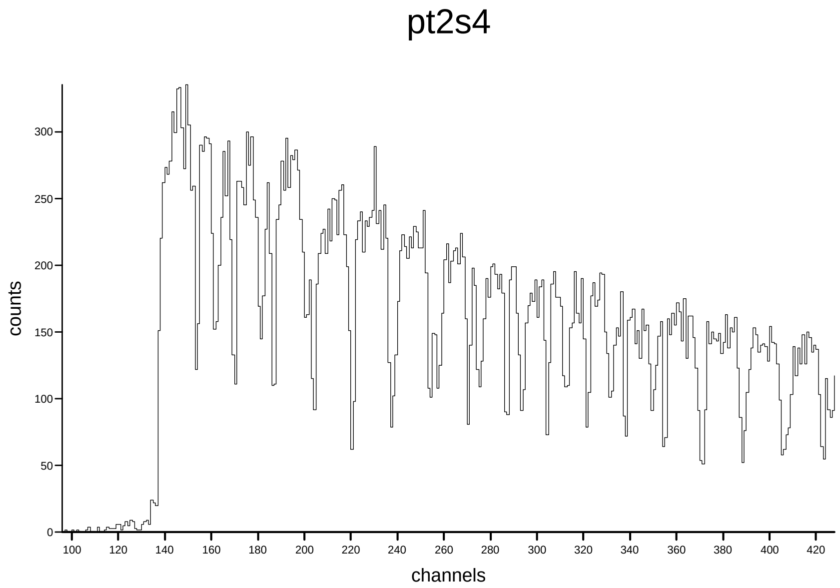


Figure 7: Expanded position spectrum for one strip. Notice the two sets of oscillations, one of slightly greater amplitude and frequency than the other. These are the shadows of the two grids on the silicon

There are two such grids within the hybrid detectors, positioned about 0.5 cm and 2.5 cm in front of the silicon. Each consists of 48 circular cross-section 0.1 mm beryllium-copper wires at a pitch of 1 mm. The range of 70 MeV $^{16}$O ions and 170 MeV $^{24}$Mg ions in such wires is rather less than this thickness, so the approximation that the wires appear as bars may be made.

A detailed examination of the position spectrum for a typical flash - gold run, without gas in the detectors, revealed that *both* sets of grids could be seen. Figure 7 shows the typical Rutherford fall off in yield with angle, with two sets of oscillations of slightly different frequency and amplitude superimposed. The deeper dips occur at a slightly higher frequency, and are therefore due to the grid nearest the silicon. The lower frequency, shallower dips are due to the other grid. The two grids are therefore forming a series of "Moiré fringes", with bars from each grid overlapping at a spacing of about 10 wires. This agrees with expectations since the two grids will form shadows of themselves on the silicon with average wire spacings inversely proportional to the target – grid distance. As shown by figure 8, this results in the observed number of fringes.

Figure 9 shows the same plot as in figure 7, except that the data shown is for a run where gas was introduced into the detectors. There is no significant difference in the spectra, suggesting that the contribution to position resolution due to ionisation straggling or multiple scattering in the gas, is essentially nil. This is true for both the 70 MeV $^{16}$O ions off a gold target and for the 170 MeV $^{24}$Mg ions from a flash - gold target.

The observation of these wires in the position spectra allowed an estimation of the position resolution of the silicon detector to be made. Initially it was suggested that the wires may appear larger than they actually are because ions might be deflected by the

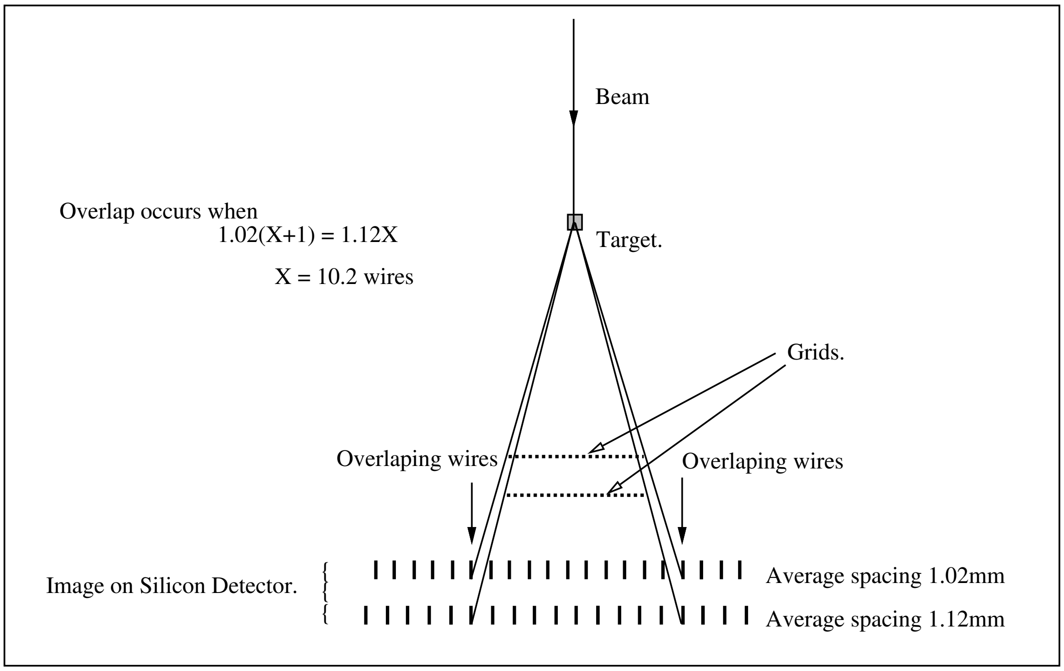


Figure 8: A schematic diagram showing how two sets of grids at different distances from the silicon can result in a series of fringes being formed. Here the projection of the grids onto the silicon is shown to result in wires from the different grids overlapping every 10 wires.

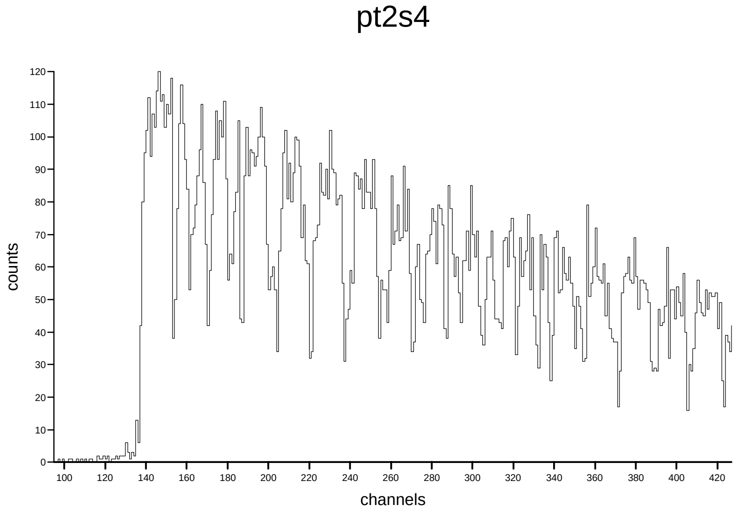


Figure 9: Position spectrum as in figure 7, except that now gas has been introduced into the detector. The similarity of the two spectra demonstrates that the effect of the gas on position resolution is negligible.

strong electric fields near the wires. The magnitude of such a deflection was estimated by first calculating the field strength near one of the wires, and then calculating the typical impulse that this would cause to a passing ion. The maximum displacement caused by this impulse was then calculated as $\approx$25 nm, small enough to ignore despite any inaccurate assumptions in the above working.

In order to make an estimate of the position resolution by consideration of the dips due to the wires, it was assumed that the shape of the dip would be the convolution of the known flat-top distribution due to the wire, folded with a Guassian distribution due to the intrinsic position response of the silicon. By measuring the FWTM of the dip, the notes of Clarke [2] could then be used to calculate the contribution from each source. This has been performed for a number of data runs, giving typical FWHM for the intrinsic position response of 0.19 mm, which is far better than the predicted resolution of $\approx$0.5mm. Coupled to the detectors being placed twice as far from the target, this would mean a great improvement in the position resolution.

A more traditional method to obtain the intrinsic position resolution is by considering the mask slits rather than the wires. The mask consisted of alternate gaps and bars of width 1.5 mm, with one of the gaps missed to allow the orientation to be determined. Using this information, the notes of Clarke were used to give typical values of 0.45 mm for the position resolution, but it should be noted that the dips made by the wires interfere with the edges of the mask slits, and hence degrade the measurements. Also, it is thought that the way the wires in the grids are manufactured results in the wires having a much cleaner profile than the bars in the mask, and hence this too may contribute to the apparent better resolution.

Another important indication as to how the silicon detectors are performing, is their intrinsic energy resolution. This has been measured by taking the FWHM of the elastics peak for 70 MeV $^{16}$O ions off a gold target. With no gas in the detector, and the energy spectrum gated on a region between two of the wires in the grids, a resolution of 258 keV was obtained. With isobutane gas introduced at a pressure of 120 torr, this increased to 525 keV. This is comparable to the energy resolution that the old psd detectors achieved. The energy lost in the gas was about 15 MeV.

The performance of the gas detector also appears to be good. In particular, the generation of particle identification spectra by the plotting of $\Delta E$ against $E$, has been shown to work very well with the hybrids. Figure 10 is such a plot for $^{24}$Mg + $^{24}$Mg data taken with a single strip, and the loci corresponding to many ion species are clearly separable.

The gas signals have also provided a method of calculating how much of the silicon is obscured by each of the grids. Figure 11 shows how there are three types of event which lead to a signal being produced in the gas detector. Type 1 events occur when an incident ion passes through only half of the gas detector before hitting one of the wires of the anode grid. These events will then have only half the expected gas signal, and no coincident silicon signal. Type 2 events are similar, except that the ions stops in the back earthing grid, generating a full $\Delta E$ signal. Only type 3 events have a full gas signal and a coincident silicon signal, and hence only these signals can be used in later analysis. Clearly, the ratios of these signals are determined by the fraction of the silicon that each of the grids obscures.

Figure 12 shows the $\Delta E$ energy spectrum for all detected events from one of the $^{24}$Mg on flash - gold runs. The small peak due to type 1 events is clearly visible, and as predicted, corresponds to exactly half the energy of the larger peak. This larger peak is presumably the sum of type 2 and type 3 events. Figure 13 is exactly the same spectrum

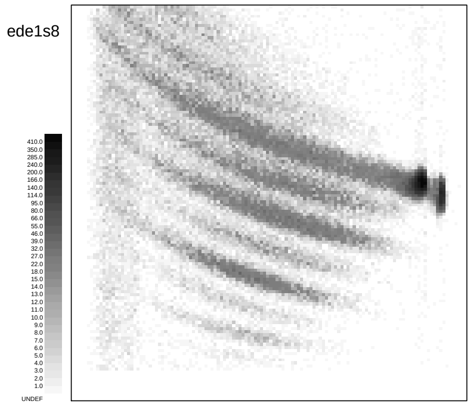


Figure 10: The particle identification spectrum for one of the new hybrid detectors for $^{24}$Mg + $^{24}$Mg data at 170 MeV.

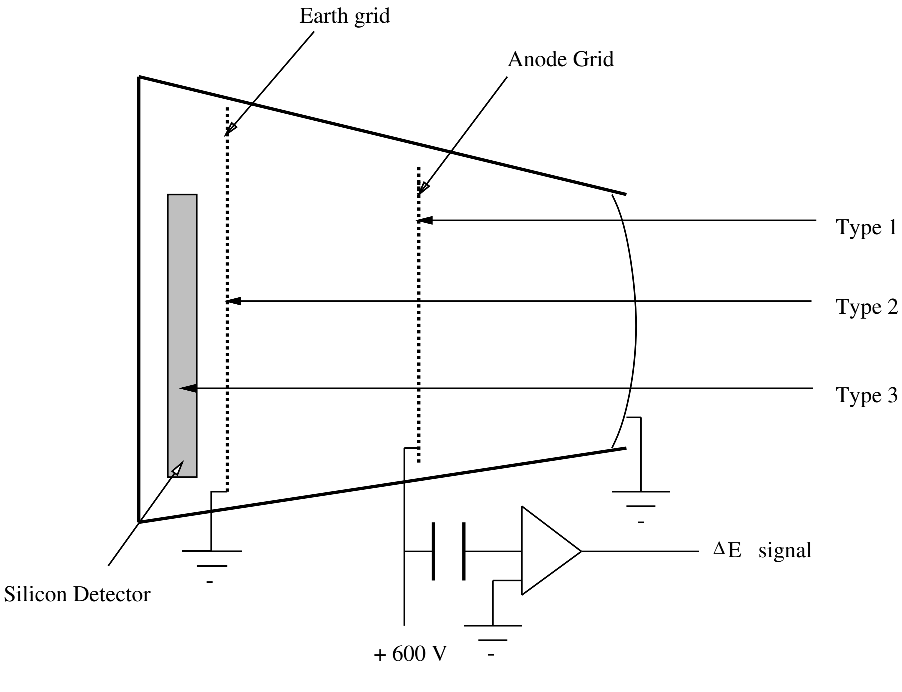


Figure 11: There are three different types of event that can give rise to a gas signal. Type 1 events occur when the incident ion stops in the anode grid, type 2 events occur when the incident ion stops in the earthing grid, and type 3 events occur when the incident ion stops in silicon detector.

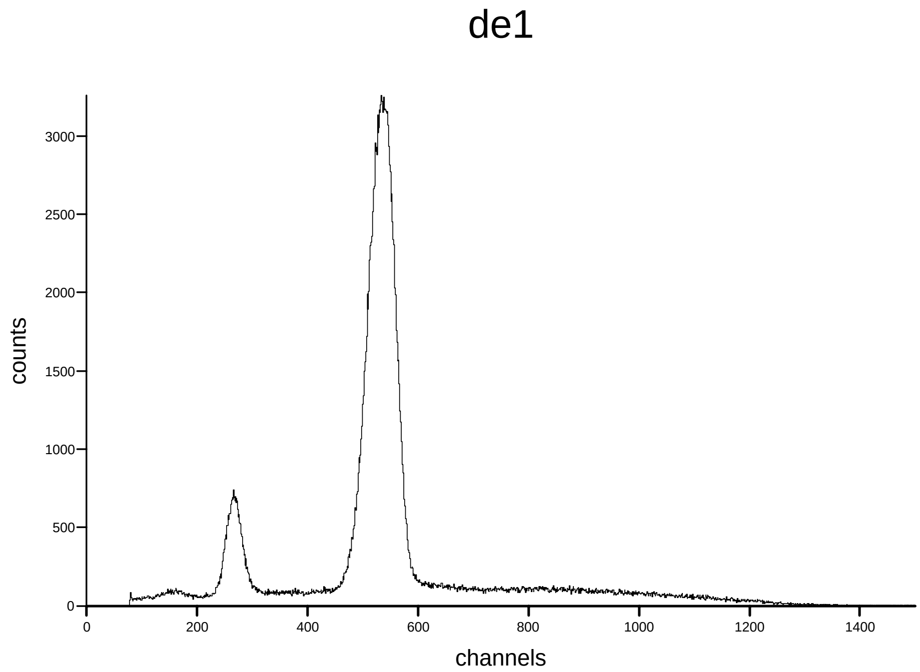


Figure 12: The energy spectrum of all $\Delta E$ signals for a $^{24}$Mg on flash - gold run.

except that this time it is only incremented if there is a coincident silicon signal. The contents of this spectrum must therefore consist entirely of type 3 events.

The number of counts in the small peak of figure 12 (the number of type 1 events) is 21620. The number of type 3 events is simply the area of the peak in figure 13, 169002, and the number of type 2 events may be calculated by subtracting the area of the large peak in figure 12 from the corresponding peak in figure 13, giving a total of 15097 type 2 events. The fraction of the silicon detector concealed by the anode grid is simply the ratio of type 1 events to the total number of events, ie. 10.5%. The ratio of the type 2 events to the total shows that the second grid obscures a futher 7.3% of incident ions, this lower figure indicating that some of the back grid is in the shadow of the front

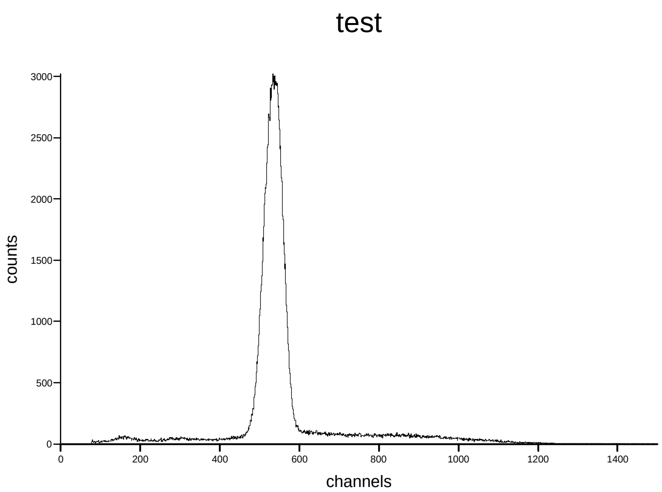


Figure 13: The same data as in figure 12 except that only signals that had a coincident signal in the silicon have been incremented.

grid. Hence only 82.2% of the detector face is infact being used. It is suggested that this worrying loss of efficiency could perhaps be reduced by using grids made of thinner wires with wider spacings between the wires.

One final aspect of the detectors' performance that has been investigated, is the effect and distribution of leakage currents across the detector. The exposure of silicon surface-barrier detectors to heavy ion radiation can cause damage to the lattice of the silicon itself, introducing trapping centres that degrade the charge collection performance of the detector. Theses trapping centres also introduce extra energy levels into the lattice, some of which will lie within the $\approx 3$ eV band gap between the valence and conduction bands, thus making it easier for thermal excitations to cause small currents within the silicon. These effects can result in electronic noise that washes out the true signals from the detector.

Three of the new gas-silicon hybrid detectors were used in the experiment, and all initially had leakage currents of about 0.2 $\mu$A. Two of the detectors were centred at 17°, and the third detector was centred at 45°. The leakage currents of the two forward detectors were found to increase rapidly, reaching leakages of about 80 $\mu$A, whereas the leakage of the third detector had increased only slightly by the end of the experiment (see figure 14). The total number of counts in each of the detectors was recorded using scalers, and indicates that the forward detectors were subject to around $10^5$ heavy ion hits per mm$^2$; about 20 times the exposure of the outer detector. It appears therefore that beam exposure is the dominant factor determining the leakage current.

The effect of this increase in leakage current upon the energy resolution of the strip detector has been examined by comparing the width of the elastics peak for flash - gold runs near the start and near the end of the experiment.

The first two runs with the 170 MeV $^{24}$Mg beam were from a flash - gold target with gas out, and with gas in. The energy resolutions for a small part of a central strip of the silicon detector were then measured as 650 keV and 970 keV respectively. By assuming that the total energy resolution is due to a component from the gas adding in quadrature with a component from the silicon, the gas contribution was found to be 720 keV. The gas in the gas detectors was constantly replaced, so no poisoning of the gas should have occurred, and hence this contribution should be constant throughout the experiment. This is confirmed by the fact that the energy spectrum of the gas signals from the flash - gold runs did not change in appearance during the experiment. The final flash - gold run gives an energy resolution of 1120 keV with the gas in, reflecting a contribution to the energy resolution from the silicon of 858 keV. These figures appear to confirm results found by Q-Par Angus Ltd [3] who give a critical exposure limit for the silicon detectors of between $10^5$ and $10^6$ heavy ion hits per mm$^2$.

After the experiment, the leakage of each of the strips of one of the forward detectors was measured individually. This was achieved by biasing up the detector in a darkened chamber and measuring the potential of each of the strips with respect to earth. The leakage was then calculated by assuming that the leakage to ground must be via the 100 k$\Omega$ resistors shown in figure 1. The results are shown in figure 15, and clearly show that it is the central strips of the detector which dominate the leakage. It was noticed that the total leakage of all 16 strips in the detector was significantly less than the 80 $\mu$A recorded at the end of the experiment. Presumably this is due to the detectors not being exposed to beam for a period of some weeks.

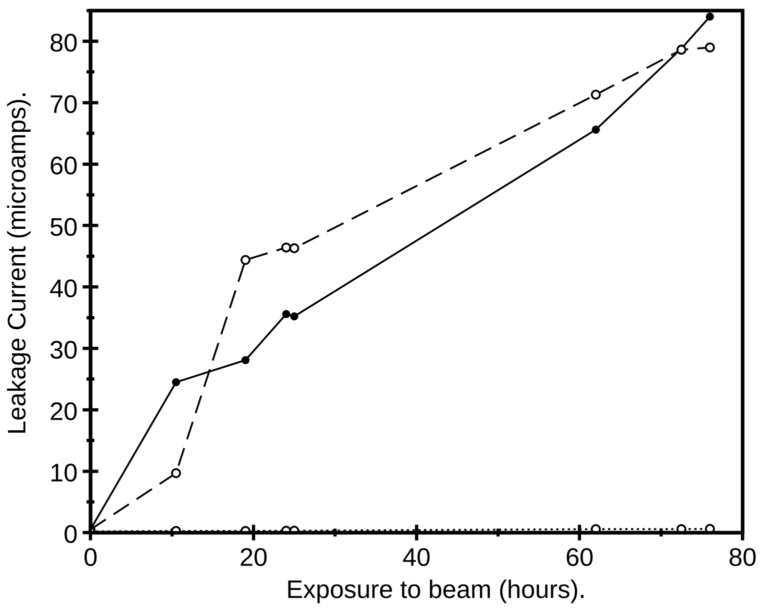


Figure 14: How the leakage currents of each of the three strip detectors varied over the duration of the experiment.

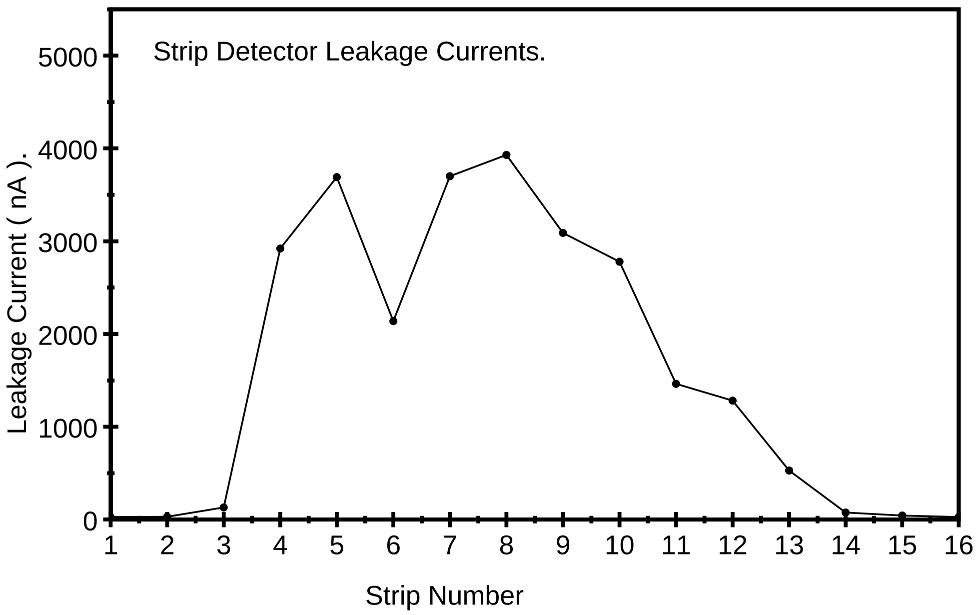


Figure 15: The leakage currents of each of the strips in one of the silicon detectors.

## Summary and Suggestions for Future Development.

An experiment has been performed at the NSF using the new gas-silicon hybrid detectors. The silicon strip detector has been shown to have an intrinsic energy response of 258 keV, and a position resolution of 0.19mm. The presence of up to 120 torr of isobutane gas in the $\Delta E$ detector has been shown not to effect the position resolution, but does increase the energy resolution to 525 keV. The energy resolution has been shown to increase only slightly due to radiation damage.

It has been suggested that the observation of the wires in of charge grids in the position spectra, might possibly form the basis for a simpler method of calibration, as opposed to the use of masks that are used at present. How these grids could be calibrated with angle by the wall mounted telescope remains unanswered. Two worrying points are noted. Firstly, the presence of the grids reduces the active area of the silicon detector by some 18%, and since later stages of analysis require coincidences between a pair of detectors, this can reduce the active area by upto 32%. This loss of efficiency could be reduced by the use of thinner wires with a wider spacing, but charge collection efficiency might then be sacrificed. Secondly, the acceptance of the yield with respect to angle is not uniform, but has a Dirac comb absorber superimposed upon it. What effect this might have upon subsequent analysis, such as the generation of $E_{rel}$ spectra and spin determinations, is unknown.

# References

[1] A. St. J. Murphy, *Search for Nuclear Molecule Configurations in* $^{48}Cr$., University of Birmingham, (1992). Unpublished.

[2] N. M. Clarke, *A Note on the Convolution of Guassians with...*, University of Birmingham, (1992). Unpublished.

[3] Q - Par Angus Ltd, Detector Test Data, (1987).